



Reactions of the σ,π -furyl complex $[\text{Fe}_2(\text{CO})_6(\mu\text{-Fu})(\mu\text{-PFu}_2)]$ (Fu = $\text{C}_4\text{H}_3\text{O}$) with phosphines: Carbonyl substitution, migratory carbonyl insertion and cyclometallation-induced furan elimination

Ahibur Rahaman^{a,b}, Fakir Rafiqul Alam^{b,c}, Shishir Ghosh^{a,d}, Derek A. Tocher^d,
Matti Haukka^e, Shariff E. Kabir^{b,**}, Ebbe Nordlander^{a,**}, Graeme Hogarth^{d,*}

^a Inorganic Chemistry Research Group, Chemical Physics, Center for Chemistry and Chemical Engineering, Lund University, Box 124, SE-221 00 Lund, Sweden

^b Department of Chemistry, Jahangirnagar University, Savar, Dhaka 1342, Bangladesh

^c Department of Chemistry, National University, Gazipur 1704, Bangladesh

^d Department of Chemistry, University College London, 20 Gordon Street, London WC1H 0AJ, UK

^e Department of Chemistry, University of Jyväskylä, Box 111, FI-40014 Jyväskylä, Finland

ARTICLE INFO

Article history:

Received 8 April 2013

Received in revised form

20 May 2013

Accepted 21 May 2013

Keywords:

Diiron

Furyl

Migratory insertion

Cyclometallation

Carbon–phosphorus bond formation

ABSTRACT

The reactivity of the σ,π -furyl complex $[\text{Fe}_2(\text{CO})_6(\mu\text{-Fu})(\mu\text{-PFu}_2)]$ (**1**) towards PPh_3 and a range of bidentate phosphines has been studied and a number of different reaction products have been identified. With PPh_3 , carbonyl substitution affords $[\text{Fe}_2(\text{CO})_5(\text{PPh}_3)(\mu\text{-Fu})(\mu\text{-PFu}_2)]$ (**2**) in which the new phosphine is coordinated to the iron center that is σ -coordinated by the bridging furyl moiety. With small bite-angle diphosphines – bis(diphenylphosphino)methane (dppm) and 1,8-bis(diphenylphosphino)naphthalene (dppn) – carbonyl substitution and migratory carbonyl insertion result to give the furyl–acyl complexes with bridging, $[\text{Fe}_2(\text{CO})_4(\mu\text{-dppm})(\mu\text{-O}=\text{C}-\text{Fu})(\mu\text{-PFu}_2)]$ (**3**), or chelating, $[\text{Fe}_2(\text{CO})_4(\kappa^2\text{-dppn})(\mu\text{-O}=\text{C}-\text{Fu})(\mu\text{-PFu}_2)]$ (**4**), diphosphines, respectively. With the more flexible diphosphines $\text{Ph}_2\text{P}(\text{CH}_2)_n\text{PPh}_2$ ($n = 2$, dppe, $n = 3$, dppp), the cyclometallated products $[\text{Fe}_2(\text{CO})_5\{\mu,\kappa^2\text{-C}_6\text{H}_4\text{PPh}(\text{CH}_2)_n\text{PPh}_2\}(\mu\text{-PFu}_2)]$ ($n = 2, 5; n = 3, \mathbf{6}$) are isolated as a result of carbonyl substitution and furan elimination, and a similar complex $[\text{Fe}_2(\text{CO})_5\{\mu,\kappa^2\text{-C}_6\text{H}_4\text{PPh}(\text{C}_6\text{H}_4)\text{PPh}_2\}(\mu\text{-PFu}_2)]$ (**7**) is generated from the more rigid diphosphine bis(diphenylphosphino)benzene (dppb). With bis(diphenylphosphino)-1,1-binaphthalene (1,1-BINAP) the novel tridentate phosphine complex $[\text{Fe}_2(\text{CO})_5\{\mu,\kappa^3\text{-C}_6\text{H}_4\text{P}(\text{C}_{20}\text{H}_{12}\text{PPh}_2)\text{C}_6\text{H}_4\text{PFu}\}]$ (**8**) results from the putative coupling of cyclometallated diphosphine and difurylphosphido ligands, following elimination of two equivalents of furan. The crystal structures of **2**, **3**, **5** and **8** have been determined and allow a detailed insight into the overall reaction profile.

© 2013 Elsevier B.V. All rights reserved.

1. Introduction

The organometallic chemistry of tri(2-furyl)phosphine (PFu_3) has been of interest as it is sterically similar to triphenylphosphine, but the electron-withdrawing nature of the 2-furyl ring makes it a poorer σ -donor than PPh_3 [1]. In a recent contribution we reported that the reaction of PFu_3 with $[\text{Fe}_3(\text{CO})_{12}]$ leads to both phosphine coordination and carbon–phosphorus bond scission to yield the σ,π -furyl complex $[\text{Fe}_2(\text{CO})_6(\mu\text{-Fu})(\mu\text{-PFu}_2)]$ (**1**) (Scheme 1) [2]. This behaviour is akin to that found for the corresponding triruthenium cluster [3,4] and this convenient route to **1** gave us the opportunity

to study the reactivity of the furyl ligand at the diiron center. Herein we describe our initial studies in this area, which have focused on the addition of mono- and bidentate phosphines. While these reactions may be expected to result in direct carbonyl substitution, it is found that a range of transformations take place, including carbonyl substitution, migratory carbonyl insertion into the metal-bound furyl ligand, reductive elimination of furan and reductive coupling of phosphorus-containing ligands.

2. Experimental

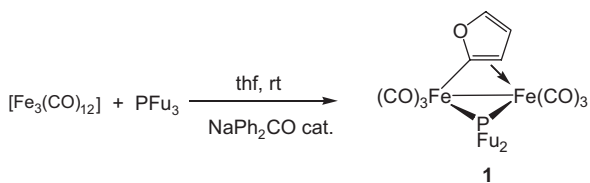
2.1. General procedures

Unless otherwise stated, purification of solvents, reactions, and manipulation of compounds were carried out under a nitrogen atmosphere with the use of standard Schlenk techniques.

* Corresponding author. Tel.: +44 (0)2076794664.

** Corresponding authors.

E-mail address: g.hogarth@ucl.ac.uk (G. Hogarth).



Scheme 1.

All solvents were dried by distillation over appropriate drying agents. All phosphine ligands were purchased from Acros Organics Chemicals Inc. and used without further purification. Complex **1** was prepared as previously reported [2]. All chromatographic separations and ensuing work-up were carried out in open air. Thin layer chromatography was carried out on glass plates pre-coated with Merck 60 0.5 mm silica gel. Infra-red spectra were recorded as solutions in 0.5 mm NaCl cells on a Nicolet Avatar 360 FT-IR-spectrometer with carbon monoxide as calibrant. Fast atom bombardment (FAB) mass spectra were obtained on a JEOL SX-102 spectrometer using 3-nitrobenzyl alcohol as matrix and CsI as calibrant. Proton and $^{31}\text{P}\{^1\text{H}\}$ NMR spectra were recorded on a Varian Unity 500 MHz NMR spectrometer.

2.2. Reaction with PPh_3

A benzene solution (20 mL) of **1** (25 mg, 0.049 mmol) and PPh_3 (13 mg, 0.049 mmol) was heated to reflux under a nitrogen atmosphere for 10 h. The solvent was removed under reduced pressure and the resultant residue was separated by TLC on silica gel. Elution with hexane/ CH_2Cl_2 (v/v 9:1) developed three bands. The faster moving band gave unreacted **1** (3 mg) and the second band gave orange $[\text{Fe}_2(\text{CO})_5(\text{PPh}_3)(\mu\text{-Fu})(\mu\text{-PFu}_2)]$ (**2**) (14 mg, 44%). A third band gave a small amount (2 mg) of a red solid tentatively formulated as $[\text{Fe}_2(\text{CO})_4(\text{PPh}_3)_2(\mu\text{-Fu})(\mu\text{-PFu}_2)]$.

Spectral and analytical data for **2**: Anal. Calcd for $\text{C}_{35}\text{H}_{24}\text{Fe}_2\text{O}_8\text{P}_2$: C, 56.32; H, 3.24. Found: C, 57.20; H, 3.52%. IR ($\nu(\text{CO})$, CH_2Cl_2): 2042 vs, 1989 vs, 1954 w cm^{-1} . ^1H NMR (CDCl_3): δ 7.61 (m, 1H, Fu), 7.30 (m, 3H, Fu), 6.50 (m, 1H, Fu), 6.35 (m, 1H, Fu), 6.10 (m, 1H, Fu), 5.79 (m, 1H, Fu), 4.03 (m, 1H, Fu), 7.26 (m, 6H, Ph), 7.21 (m, 9H, Ph). $^{31}\text{P}\{^1\text{H}\}$ NMR (CDCl_3): δ 67.7 (brs), 71.7 (brs). ESI-MS: m/z 746 $[\text{M}]^+$.

2.3. Reaction with bis(diphenylphosphino)methane (dppm)

A benzene solution (20 mL) of **1** (30 mg, 0.059 mmol) and dppm (23 mg, 0.059 mmol) was refluxed under a nitrogen atmosphere for 12 h. The solvent was removed under reduced pressure and the residue was chromatographed by TLC on silica gel. Elution with cyclohexane/ CH_2Cl_2 (9:1 v/v) developed two bands. The faster band was unreacted **1** (4 mg) while the slower band afforded $[\text{Fe}_2(\text{CO})_4(\mu\text{-dppm})(\mu\text{-O=C-Fu})(\mu\text{-PFu}_2)]$ (**3**) (15 mg, 34%) as red crystals after recrystallization from hexane/ CH_2Cl_2 at 4 °C. Spectral data for **3**: Anal. Calcd for $\text{C}_{42}\text{H}_{31}\text{Fe}_2\text{O}_8\text{P}_2$: C, 58.09; H, 3.60. Found: C, 58.62; H, 3.86%. IR ($\nu(\text{CO})$, CH_2Cl_2): 1990 s, 1961 vs, 1926 m, 1913 sh cm^{-1} . ^1H NMR (CDCl_3): δ 2.71 (ddd, $J = 19.5, 10.5, 9.0$ Hz, 1H), 3.51–3.59 (m, 1H), 6.01–6.013 (m, 1H, Fu), 6.03 (d, $J = 3.5$ Hz, 1H, Fu), 6.20–6.21 (m, 1H, Fu), 6.40 (dd, $J = 3.0, 1.5$ Hz, 1H, Fu), 6.60 (br, 1H, Fu), 6.75 (d, $J = 3.0$ Hz, 1H, Fu), 6.95 (s, 1H, Fu), 7.57 (s, 1H, Fu), 7.61 (s, 1H, Fu), 7.06–7.07 (m, 3H, Ph), 7.11–7.15 (m, 2H, Ph), 7.23–7.29 (m, 6H, Ph), 7.34–7.37 (m, 5H, Ph), 7.42–7.47 (m, 4H, Ph). $^{31}\text{P}\{^1\text{H}\}$ NMR (CDCl_3): δ 136.3 (dd, $J = 115, 59$ Hz), 54.4 (t, $J = 115$ Hz), 43.4 (dd, $J = 115, 59$ Hz).

2.4. Reaction with 1,8-bis(diphenylphosphino)naphthalene (dppn)

A benzene solution (20 mL) of **1** (25 mg, 0.049 mmol) and dppn (24.2 mg, 0.049 mmol) was refluxed under a nitrogen atmosphere for

12 h. The solvent was removed under reduced pressure and the residue was chromatographed by TLC on silica gel. Elution with cyclohexane/ CH_2Cl_2 (9:1 v/v) developed two bands. The faster band was unreacted **1** (3 mg) while the slower band afforded $[\text{Fe}_2(\text{CO})_4(\kappa^2\text{-dppn})(\mu\text{-O=C-Fu})(\mu\text{-PFu}_2)]$ (**4**) (12 mg, 34%) as red crystals after recrystallization from hexane/ CH_2Cl_2 at 4 °C. Spectral data for **4**: Anal. Calcd for $\text{C}_{51}\text{H}_{35}\text{Fe}_2\text{O}_8\text{P}_2$: C, 62.47; H, 3.61. Found: C, 62.70; H, 3.95%. IR ($\nu(\text{CO})$, CH_2Cl_2): 2010 vs, 1954 s, 1941 w cm^{-1} . ^1H NMR (CDCl_3): δ 6.49 (m, 3H, Fu), 7.01 (m, 6H, Fu), 7.15–7.41 (m, 20H, Ph), 7.67–7.43 (m, 6H). $^{31}\text{P}\{^1\text{H}\}$ NMR (CDCl_3): δ 61.5 (t, $J = 19$ Hz), 59.1 (d, $J = 19$ Hz), 58.6 (d, $J = 19$ Hz). ESI-MS: m/z 980 $[\text{M}]^+$.

2.5. Reaction with bis(diphenylphosphino)ethane (dppe)

A benzene solution (20 mL) of **1** (30 mg, 0.059 mmol) and dppe (23.5 mg, 0.059 mmol) was refluxed under a nitrogen atmosphere for 12 h. The solvent was removed under reduced pressure and the residue was chromatographed by TLC on silica gel. Elution with cyclohexane/ CH_2Cl_2 (9:1 v/v) developed three bands. The faster band was unreacted **1** (4 mg) and the slower band afforded $[\text{Fe}_2(\text{CO})_5\{\mu\text{-}\kappa^2\text{-C}_6\text{H}_4\text{PPh}(\text{CH}_2)_2\text{PPh}_2\}(\mu\text{-PFu}_2)]$ (**5**) (15 mg, 41%) as red crystals after recrystallization from hexane/ CH_2Cl_2 at 4 °C. Spectral data for **5**: Anal. Calcd for $\text{C}_{39}\text{H}_{29}\text{Fe}_2\text{O}_7\text{P}_2$: C, 57.52; H, 3.60. Found: C, 57.62; H, 3.88%. IR ($\nu(\text{CO})$, CH_2Cl_2): 2038 s, 1982 vs, 1941 w cm^{-1} . ^1H NMR (CDCl_3): δ 2.62–2.66 (m, 2H), 2.88–2.94 (m, 2H), 6.10 (m, 1H, Fu), 6.15 (m, 1H, Fu), 6.19–6.20 (m, 1H, Fu), 6.21 (m, 1H, Fu), 6.72–6.75 (m, 1H, Fu), 6.79–6.82 (m, 1H, Fu), 7.13–7.31 (m, 14H, Ph), 7.45–7.48 (m, 3H, Ph), 7.59–7.63 (m, 1H, Ph), 7.99–8.03 (m, 1H, Ph). $^{31}\text{P}\{^1\text{H}\}$ NMR (CDCl_3): δ 101.0 (dd, $J = 134, 15$ Hz), 83.9 (dd, $J = 134, 19$ Hz), 81.0 (t, $J = 17$ Hz).

2.6. Reaction with bis(diphenylphosphino)propane (dppp)

A benzene solution (20 mL) of **1** (30 mg, 0.059 mmol) and dppp (24 mg, 0.059 mmol) was refluxed under a nitrogen atmosphere for 11 h. The solvent was removed under reduced pressure and the residue was chromatographed by TLC on silica gel. Elution with cyclohexane/ CH_2Cl_2 (9:1 v/v) developed two bands. The faster band was unreacted **1** (3 mg) while the slower band afforded $[\text{Fe}_2(\text{CO})_5\{\mu\text{-}\kappa^2\text{-C}_6\text{H}_4\text{PPh}(\text{CH}_2)_3\text{PPh}_2\}(\mu\text{-PFu}_2)]$ (**6**) (12 mg, 31%) as red crystals after recrystallization from hexane/ CH_2Cl_2 at 4 °C. Spectral data for **6**: Anal. Calcd for $\text{C}_{40}\text{H}_{31}\text{Fe}_2\text{O}_7\text{P}_2$: C, 57.98; H, 3.78. Found: C, 58.62; H, 3.98%. IR ($\nu(\text{CO})$, CH_2Cl_2): 2043 s, 1987 vs, 1941 w cm^{-1} . ^1H NMR (CDCl_3): δ 1.8–2.00 (m, 2H), 2.22–2.6 (m, 2H), 3.8–4.1 (m, 2H), 6.15 (m, 1H, Fu), 6.32 (m, 2H, Fu), 6.48 (m, 1H, Fu), 6.40 (m, 1H, Fu), 6.5 (m, 1H, Fu), 7.10–7.54 (m, 19H, Ph). $^{31}\text{P}\{^1\text{H}\}$ NMR (CDCl_3): δ 73.5 (br), 56.4 (brs), 31.9 (d, $J = 116$ Hz).

2.7. Reaction with 1,2-bis(diphenylphosphino)benzene (dppb)

A toluene solution (20 mL) of **1** (22 mg, 0.043 mmol) and dppb (18 mg, 0.043 mmol) was refluxed under a nitrogen atmosphere for 27 h. The solvent was removed under reduced pressure and the residue was chromatographed by TLC on silica gel. Elution with cyclohexane/ CH_2Cl_2 (4:1 v/v) developed two bands. The faster band was unreacted **1** (2 mg) while the slower moving band afforded $[\text{Fe}_2(\text{CO})_5\{\mu\text{-}\kappa^2\text{-C}_6\text{H}_4\text{PPh}(\text{C}_6\text{H}_4)\text{PPh}_2\}(\mu\text{-PFu}_2)]$ (**7**) (20 mg, 66%) as red crystals after recrystallization from hexane/ CH_2Cl_2 at 4 °C. Spectral data for **7**: Anal. Calcd for $\text{C}_{39}\text{H}_{29}\text{Fe}_2\text{O}_7\text{P}_2$: C, 57.52; H, 3.60. Found: C, 57.62; H, 3.88%. IR ($\nu(\text{CO})$, CH_2Cl_2): 2023 s, 1983 vs, 1945 w cm^{-1} . ^1H NMR (CDCl_3): δ 5.72–5.63 (m, 1H, Fu), 6.08 (m, 1H, Fu), 6.20 (m, 1H, Fu), 6.29 (m, 2H, Fu), 6.31 (m, 1H, Fu), 6.53–6.41 (m, 2H, Ph), 6.83–6.80 (m, 3H, Ph), 7.18–7.10 (m, 5H, Ph), 7.48–7.30 (m, 9H, Ph), 7.96–7.62 (m, 4H, Ph). $^{31}\text{P}\{^1\text{H}\}$ NMR (CDCl_3): δ 138.7 (dd, $J = 54, 30$ Hz), 90.5 (t, $J = 55$ Hz), 82.7 (dd, $J = 50, 30$ Hz).

2.8. Reaction with bis(diphenylphosphino)-1,1'-binaphthalene (BINAP)

A toluene solution (20 mL) of **1** (20 mg, 0.039 mmol) and BINAP (24 mg, 0.039 mmol) was refluxed under a nitrogen atmosphere for 24 h. The solvent was removed under reduced pressure and the residue was chromatographed by TLC on silica gel. Elution with cyclohexane/CH₂Cl₂ (3:2 v/v) developed two bands. The faster band was unreacted **1** (5 mg) while the slower band afforded [Fe₂(CO)₅{μ,κ³-C₆H₄P(C₂₀H₁₂PPh₂)C₆H₄PFu}] (**8**) (5 mg, 18%) as red crystals after recrystallization from hexane/CH₂Cl₂ at 4 °C. Spectral data for **8**: IR (ν(CO), CH₂Cl₂): 2043 s, 2023 m, 1981 vs, 1954 w cm⁻¹. ¹H NMR (CDCl₃): δ 5.22 (m, 1H), 5.38 (m, 4H), 5.68 (m, 2H), 6.32 (m, 1H), 6.49 (m, 1H), 6.74 (m, 2H), 7.18 (m, 9H), 7.30 (m, 7H), 7.48 (m, 2H), 7.74 (m, 3H). ³¹P{¹H} NMR (CDCl₃): δ 154.4 (dd, *J* = 57, 34 Hz), 90.7 (dd, *J* = 57, 34 Hz), 64.4 (t, *J* = 57 Hz).

2.9. X-ray crystallography

Single crystals of **3** and **5** were mounted on fibres and diffraction data collected on a Bruker SMART APEX diffractometer at 150 K using Mo-Kα radiation (λ = 0.71073 Å). Data collection, indexing and initial cell refinements were all done using SMART software. Data reduction was accomplished with SAINT software [5] and SADABS [6] programs were used to apply empirical absorption corrections. The structures were solved by direct methods and refined by a full matrix least-squares method. All non-hydrogen atoms were refined anisotropically and hydrogen atoms were included using a riding model. Scattering factors were taken from the International Tables for X-ray Crystallography. For **3**, which

crystallises in the orthorhombic space group P2₁2₁2₁, the absolute structure parameter was -0.008(10). Single crystals of **2** and **8** were immersed in cryo-oil, mounted in a Nylon loop, and measured at 120 K and 150 K, respectively. The X-ray diffraction data was collected on a Bruker Kappa Apex II Duo diffractometer using Mo-Kα radiation (λ = 0.71073 Å). The APEX2 [7] program package was used for cell refinements and data reductions. The structure was solved by direct methods using the SHELXS-86 (**2**) [8] or SHELXS-97 (**8**) [9] program with the WinGX [10] graphical user interface. A multi-scan absorption correction based on equivalent reflections (SADABS) [6] was applied to the data. Structural refinement was carried out using SHELXL-97. In **8**, the electron density due to the solvent of crystallization could not be unambiguously resolved and it was equated to one dichloromethane and one n-hexane molecules by using the SQUEEZE routine of PLATON [11]. The missing solvent was taken into account in the unit cell content. The hydrogen atoms were positioned geometrically and constrained to ride on their parent atoms, with C-H = 0.95–1.00 Å, B-H = 1.12 Å, and *U*_{iso} = 1.2–1.5 *U*_{eq} (parent atom). Details of data collection and structure refinement are given in Table 1.

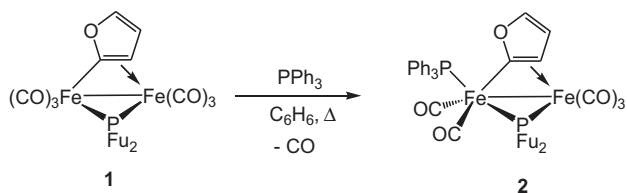
3. Results and discussion

3.1. Reaction of **1** with PPh₃ – formation of the carbonyl substitution product [Fe₂(CO)₅(PPh₃)(μ-Fu)(μ-PFu₂)] (**2**)

Heating a benzene solution of **1** with an equimolar amount of PPh₃ for 10 h resulted in the isolation of the carbonyl substitution product [Fe₂(CO)₅(PPh₃)(μ-Fu)(μ-PFu₂)] (**2**) in 44% yield after chromatography (Scheme 2). Characterization was relatively

Table 1
Crystal data and experimental details for [Fe₂(CO)₅(PPh₃)(μ-Fu)(μ-PFu₂)] (**2**), [Fe₂(CO)₄(μ-dppm)(μ-O=C-Fu)(μ-PFu₂)] (**3**), [Fe₂(CO)₅{μ,κ²-C₆H₄PPh(CH₂)₂PPh₂}(μ-PFu₂)] (**5**), [Fe₂(CO)₅{μ,κ³-C₆H₄P(C₂₀H₁₂PPh₂)C₆H₄PFu}] (**8**).

Compound	2	3	5	8
Empirical formula	C ₃₅ H ₂₄ O ₈ Fe ₂ P ₂	C ₄₂ H ₃₁ O ₈ Fe ₂ P ₃	C ₃₉ H ₂₉ O ₇ Fe ₂ P ₃	C ₆₀ H ₄₇ O ₆ Fe ₂ P ₃ Cl ₂
Formula weight	746.18	868.28	814.238	1139.49
Temp (K)	120(2)	150(2)	150(2)	150(2)
Wavelength (Å)	0.71073	0.71073	0.71073	0.71073
Crystal system	Monoclinic	Orthorhombic	Triclinic	Triclinic
Space group	P2 ₁ /c	P2 ₁ 2 ₁ 2 ₁	P 1 bar	P 1 bar
<i>a</i> (Å)	10.0094(4)	9.807(2)	9.443(1)	11.3018(6)
<i>b</i> (Å)	30.993(1)	18.617(3)	11.135(2)	13.1349(7)
<i>c</i> (Å)	12.5811(4)	20.920(4)	17.781(2)	17.819(1)
α (°)	90	90	105.656(2)	106.003(2)
β (°)	124.796(2)	90	90.651(2)	101.143(2)
γ (°)	90	90	95.419(2)	94.570(2)
Volume (Å ³)	3205.0(2)	3819(1)	1790.9(4)	2469.8(2)
<i>Z</i>	4	4	24	2
<i>D</i> _{calc} (Mg m ⁻³)	1.546	1.510	1.510	1.532
μ (Mo Kα) (mm ⁻¹)	1.058	0.940	0.994	0.849
<i>F</i> (000)	1520	1776	832	1172
Crystal colour	Red	Red	Red	Red
Crystal size (mm)	0.27 × 0.21 × 0.16	0.46 × 0.16 × 0.04	0.46 × 0.19 × 0.04	0.28 × 0.26 × 0.21
θ range (°)	2.08–30.00	2.29–28.24	2.38–28.31	1.86–25.50
Limiting indices	-14 ≤ <i>h</i> ≤ 13 -43 ≤ <i>k</i> ≤ 40 -17 ≤ <i>l</i> ≤ 17	-12 ≤ <i>h</i> ≤ 12 -23 ≤ <i>k</i> ≤ 23 -27 ≤ <i>l</i> ≤ 26	-12 ≤ <i>h</i> ≤ 12 -14 ≤ <i>k</i> ≤ 14 -22 ≤ <i>l</i> ≤ 22	-13 ≤ <i>h</i> ≤ 13 -15 ≤ <i>k</i> ≤ 15 0 ≤ <i>l</i> ≤ 21
Structure solution	Direct methods	Direct methods	Direct methods	Direct methods
Reflections collected	47,305	31,859	14,903	9098
Independent reflections (<i>R</i> _{int})	9326 (0.0252)	8908 (0.0497)	7879 (0.0276)	9098 (0.0361)
Max. and min. transmission	0.8532 and 0.7668	0.9634 and 0.6718	0.9613 and 0.6577	0.8426 and 0.7946
Data/restraints/parameters	9326/0/424	8908/0/496	7879/0/460	9098/0/577
Goodness of fit on <i>F</i> ²	1.032	0.996	1.040	1.076
Final <i>R</i> indices [<i>I</i> > 2σ(<i>I</i>)]	<i>R</i> ₁ = 0.0305 <i>wR</i> ₂ = 0.0682	<i>R</i> ₁ = 0.0354 <i>wR</i> ₂ = 0.0761	<i>R</i> ₁ = 0.0513 <i>wR</i> ₂ = 0.1315	<i>R</i> ₁ = 0.0505 <i>wR</i> ₂ = 0.1296
<i>R</i> indices (all data)	<i>R</i> ₁ = 0.0423 <i>wR</i> ₂ = 0.0723	<i>R</i> ₁ = 0.0430 <i>wR</i> ₂ = 0.0800	<i>R</i> ₁ = 0.0670 <i>wR</i> ₂ = 0.1451	<i>R</i> ₁ = 0.0840 <i>wR</i> ₂ = 0.1427
Largest peak and hole (e Å ⁻³)	0.544 and -0.470	0.602 and -0.305	1.231 and -0.366	0.838 and -0.497



Scheme 2.

straightforward with IR spectra being particularly informative of the degree of carbonyl substitution, the highest frequency carbonyl vibration at 2042 cm^{-1} being characteristic of a $\text{Fe}_2(\text{CO})_5\text{L}$ framework. The ^1H NMR displayed a multiplet at δ 4.03 that is assigned to the proton attached to the β -carbon of the furyl ligand, the chemical shift being quite characteristic, while other furyl and phenyl protons were observed between δ 7.6–5.8. The $^{31}\text{P}\{^1\text{H}\}$ NMR spectrum consisted of two broad singlets at 71.7 and 67.7 ppm, suggesting that the complex is fluxional in solution. In order to elucidate the position of phosphine substitution and also to confirm that the furyl ligand was still intact (see below), a single crystal X-ray diffraction study of **2** was carried out, the results of which are summarized in Fig. 1 and its caption.

The gross structural features of **2** are similar to those in **1** and the substituted analogue $[\text{Fe}_2(\text{CO})_5(\text{PFu}_3)(\mu\text{-Fu})(\mu\text{-PFu}_2)]$ (**2-PFu₃**) [2]. The iron–iron vector of 2.5884(3) Å is spanned by furyl and difurylphosphido ligands in relative *cis* disposition. Unlike the above-mentioned PFu_3 derivative, in which the phosphine is coordinated to the π -bound iron atom [2], the triphenylphosphine ligand in **2** is coordinated to the σ -bound iron atom, lying approximately *trans* to the iron–iron vector [$\text{Fe}(2)\text{--Fe}(1)\text{--P}(2)$ 143.55(1) $^\circ$]. In previous work we have considered the nature of the alkenyl bonding to the diiron center through the parameters ΔC_α and ΔFe_π , defined as $\{(\text{Fe}_\pi\text{--}C_\alpha) - (\text{Fe}_\sigma\text{--}C_\alpha)\}$ and $\{(\text{Fe}_\pi\text{--}C_\alpha) - (\text{Fe}_\pi\text{--}C_\beta)\}$, respectively [12], with ΔC_α being a measure of how symmetrically the α -carbon bridges the diiron center and ΔFe_π differentiating between metalla-olefin and metallacyclic binding modes [12]. For **1** and **2-PFu₃** ΔC_α values of 0.172(4)–0.223(4) Å are significantly

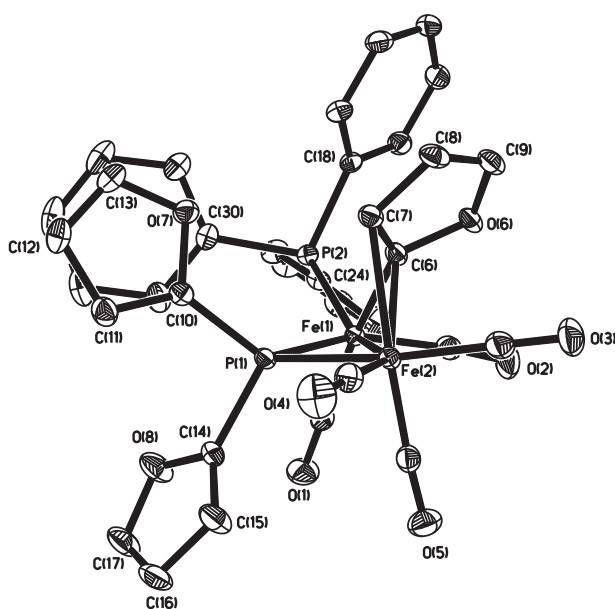


Fig. 1. Molecular structure of $[\text{Fe}_2(\text{CO})_5(\text{PPh}_3)(\mu\text{-Fu})(\mu\text{-PFu}_2)]$ (**2**) with selected bond lengths (Å) and angles ($^\circ$): $\text{Fe}(1)\text{--Fe}(2)$ 2.5884(3), $\text{Fe}(1)\text{--P}(2)$ 2.2219(4), $\text{Fe}(1)\text{--C}(6)$ 1.958(2), $\text{Fe}(2)\text{--C}(7)$ 2.303(2), $\text{Fe}(2)\text{--C}(6)$ 2.151(2), $\text{Fe}(1)\text{--Fe}(2)\text{--P}(2)$ 143.55(1).

larger than those of around 0.1 Å for simple aryl- or alkyl-substituted diiron–alkenyl complexes and the value of 0.193(4) Å in **2** underscores the idea that furyl (and thienyl) are special examples of σ,π -alkenyl ligands.

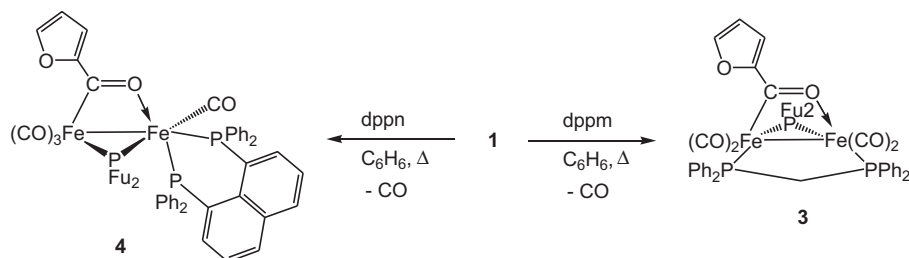
The reaction of **1** with PPh_3 is akin to that of the ruthenium analogue $[\text{Ru}_2(\text{CO})_6(\mu\text{-Fu})(\mu\text{-PFu}_2)]$ (**1-Ru**) which also yields the substitution product $[\text{Ru}_2(\text{CO})_5(\text{PPh}_3)(\mu\text{-Fu})(\mu\text{-PFu}_2)]$ (**2-Ru**) although the required reaction conditions and yields vary significantly [13]. Thus **2-Ru** is formed in high yield upon simply stirring **1-Ru** and PPh_3 in dichloromethane in a reaction that has been shown to be associative in nature [13]. The more forcing conditions required for formation of **2** and the low isolated yields suggest that this transformation is more likely to be of a dissociative nature, but further studies are needed in order to assess the mechanism of this substitution reaction.

3.2. Reaction of **1** with bis(diphenylphosphino)methane (dppm) and 1,8-bis(diphenylphosphino)naphthalene (dppn) – formation of the migratory carbonyl insertion products $[\text{Fe}_2(\text{CO})_4(\mu\text{-dppm})(\mu\text{-O=C-Fu})(\mu\text{-PFu}_2)]$ (**3**) and $[\text{Fe}_2(\text{CO})_4(\kappa^2\text{-dppn})(\mu\text{-O=C-Fu})(\mu\text{-PFu}_2)]$ (**4**)

Heating a benzene solution of **1** and dppm for 12 h led to the isolation of $[\text{Fe}_2(\text{CO})_4(\mu\text{-dppm})(\mu\text{-O=C-Fu})(\mu\text{-PFu}_2)]$ (**3**) in 34% yield as the sole reaction product (Scheme 3). The IR spectrum of **3** is characteristic of a $\text{Fe}_2(\text{CO})_4\text{L}_2$ bridge framework in which the diphosphine spans the metal–metal bond, the highest frequency carbonyl vibration appearing at 1990 cm^{-1} . In the $^{31}\text{P}\{^1\text{H}\}$ NMR spectrum, three well-resolved signals are observed at 43.4, 54.4 and 136.3 ppm, showing that the diiron center is unsymmetrically bridged – the low-field signal being assigned to the difurylphosphido bridge. The ^1H NMR spectrum showed a pair of high-field multiplets at δ 2.71 and 3.55 characteristic of the methylene protons on the diphosphine, but all other signals appeared downfield of 6 ppm, suggesting that the furyl ligand is not bridging the diiron center. In order to elucidate the nature of the bridging ligand, the structure of **3** was determined by a single crystal X-ray diffraction study, the results of which are summarized in Fig. 2 and its caption.

The diphosphine bridges the diiron center, lying approximately *trans* to the difurylphosphido moiety [$\text{P}(1)\text{--Fe}(1)\text{--P}(2)$ 141.80(3), $\text{P}(1)\text{--Fe}(2)\text{--P}(3)$ 152.05(3) $^\circ$] and, at approximately right angles to both, lies a furyl–acyl ligand that most likely is the result of carbonyl insertion into the metal-bound furyl ligand. The bridging carbonyl moiety is characterized by iron–carbon and iron–oxygen distances of 1.935(2) Å [$\text{Fe}(1)\text{--C}(6)$] and 1.998(2) Å [$\text{Fe}(2)\text{--O}(5)$], and the furyl group lies approximately in the Fe_2CO plane, suggesting that there is electronic delocalization/conjugation between the acyl and furyl moieties. The $\text{C}(6)\text{--O}(5)$ bond length of 1.270(3) Å compares well with related diiron acyl complexes [14–17].

Similarly, reaction of **1** with 1,8-bis(diphenylphosphino)naphthalene (dppn) results in the loss of one carbonyl and insertion of a second into the diiron–furyl subunit to afford $[\text{Fe}_2(\text{CO})_4(\kappa^2\text{-dppn})(\mu\text{-O=C-Fu})(\mu\text{-PFu}_2)]$ (**4**) in 34% yield (Scheme 3). The key difference between **3** and **4** is that in the latter the diphosphine binds in a chelating fashion to a single iron atom. This is clearly seen from the IR spectrum, where the carbonyl region consists of three absorptions at 2010 vs, 1954 s and 1941 m cm^{-1} , the positions and pattern of which is characteristic of an $\text{Fe}_2(\text{CO})_4\text{L}_2$ chelate framework. The diphosphine can potentially chelate to either the oxygen- or carbon-bound iron atom but it is known that the former is favoured. For example, in closely related work, we have shown by X-ray crystallography that in both $[\text{Fe}_2(\text{CO})_4(\kappa^2\text{-dippe})(\mu\text{-O=C-Th})(\mu\text{-PTh}_2)]$ and $[\text{Fe}_2(\text{CO})_4(\kappa^2\text{-dppb})(\mu\text{-O=C-Th})(\mu\text{-PTh}_2)]$ the diphosphine is coordinated to the oxygen-bound iron atom [18]. Assuming that this is the case for **4**, three geometric isomers are possible.



Scheme 3.

The $^{31}\text{P}\{^1\text{H}\}$ NMR spectrum of **4** indicates that only one geometric isomer is formed. Three sharp signals are seen, an apparent triplet at 61.5 ppm ($J = 19$ Hz) and a pair of doublets at 59.1 and 58.6 ppm. We assign the (apparent) triplet resonance to the difurylphosphido-bridge, the lack of any large couplings suggesting that the isomer shown in Scheme 3 is selectively adopted, i.e. a structure with the bulky diphosphine occupying equatorial sites in a distorted trigonal bipyramidal metal center, with the carbonyl and phosphido groups occupying the axial positions.

In light of the isolation of the carbonyl substitution product **2** from the reaction of triphenylphosphine with **1**, it is tempting to speculate that formation of **3** and **4** results *via* the intermediate formation of monodentate complexes bearing a dangling phosphine moiety. Coordination of this free phosphine moiety would then lead to migratory carbonyl insertion to give the observed products based on the known propensity for dppm to bridge metal atoms [19] and dppn to act as a chelating ligand [20]. This is akin to the behaviour noted previously for $[\text{Fe}_2(\text{CO})_6(\mu\text{-HC=CHPh})(\mu\text{-PPh}_2)]$ in which the intermediate monodentate dppm complex, $[\text{Fe}_2(\text{CO})_5(\kappa^1\text{-dppm})(\mu\text{-HC=CHPh})(\mu\text{-PPh}_2)]$, was isolated and shown to transform into the vinyl–acyl complex $[\text{Fe}_2(\text{CO})_4(\mu\text{-dppm})(\mu\text{-O=C-HC=CHPh})(\mu\text{-PPh}_2)]$ upon further heating [17].

Wong and co-workers have studied the reaction of the di-ruthenium analogue $[\text{Ru}_2(\text{CO})_6(\mu\text{-Fu})(\mu\text{-PFu}_2)]$ (**1-Ru**) with dppm and related diphosphines that are known to bridge metal–metal bonds [21]. For the diruthenium complex, carbonyl substitution takes place in all cases; for example, with dppm the sole product is $[\text{Ru}_2(\text{CO})_4(\mu\text{-dppm})(\mu\text{-Fu})(\mu\text{-PFu}_2)]$ that has been crystallographically characterized. It is not clear whether addition of the second phosphorus atom at the diruthenium center is a straight-forward substitution process or occurs *via* initial migratory insertion to give $[\text{Ru}_2(\text{CO})_4(\mu\text{-dppm})(\mu\text{-O=C-Fu})(\mu\text{-PFu}_2)]$ that subsequently loses the inserted carbonyl. Carbonyl loss from binuclear vinyl–acyl complexes has been documented [16] and is facile for diiron–thiolate complexes but less so for related phosphido-bridged complexes.

3.3. Reaction of **1** with 1,2-bis(diphenylphosphino)ethane (dppe), 1,3-bis(diphenylphosphino)propane (dppp) and 1,2-bis(diphenylphosphino)benzene (dppb) – orthometallation and furan loss to give $[\text{Fe}_2(\text{CO})_5\{\mu,\kappa^2\text{-C}_6\text{H}_4\text{PPh}(\text{CH}_2)_n\text{PPh}_2\}(\mu\text{-PFu}_2)]$ ($n = 2$, **5**; $n = 3$, **6**) and $[\text{Fe}_2(\text{CO})_5\{\mu,\kappa^2\text{-C}_6\text{H}_4\text{PPh}(\text{C}_6\text{H}_4)\text{PPh}_2\}(\mu\text{-PFu}_2)]$ (**7**)

Reactions of **1** with 1,2-bis(diphenylphosphino)ethane (dppe) in refluxing benzene afforded $[\text{Fe}_2(\text{CO})_5\{\mu,\kappa^2\text{-C}_6\text{H}_4\text{PPh}(\text{CH}_2)_2\text{PPh}_2\}(\mu\text{-PFu}_2)]$ (**5**) in 41% yield after workup, while a similar reaction with 1,3-bis(diphenylphosphino)propane (dppp) yielded $[\text{Fe}_2(\text{CO})_5\{\mu,\kappa^2\text{-C}_6\text{H}_4\text{PPh}(\text{CH}_2)_3\text{PPh}_2\}(\mu\text{-PFu}_2)]$ (**6**) in 31% yield. In a similar manner, heating **1** and 1,2-bis(diphenylphosphino)benzene (dppb) in toluene gave $[\text{Fe}_2(\text{CO})_5\{\mu,\kappa^2\text{-C}_6\text{H}_4\text{PPh}(\text{C}_6\text{H}_4)\text{PPh}_2\}(\mu\text{-PFu}_2)]$ (**7**) in 66% yield (Scheme 4). While it was clear from the IR spectra that **5**–**7** contained an $\text{Fe}_2(\text{CO})_5\text{L}_2$ core, and from the $^{31}\text{P}\{^1\text{H}\}$ NMR spectra that the three phosphorus atoms were metal-bound, their structures only became apparent following an X-ray crystallographic study of **5**, the results of which are summarized in Fig. 3 and its caption.

The diiron unit is still spanned by a difurylphosphido ligand but the furyl moiety has been lost and one of the iron atoms is instead bound to an orthometallated phenyl ring from the diphosphine. The latter chelates to one metal center *via* both phosphorus atoms $[\text{P}(2)\text{-Fe}(2)\text{-P}(3) 85.28(3)^\circ]$ and spans the diiron center *via* the orthometallated phenyl ligand $[\text{C}(14)\text{-Fe}(2) 2.042(3) \text{ \AA}]$. In accommodating this new ligand, the iron–iron bond of 2.7639(6) Å in **5** is significantly elongated with respect to those in **2** and **3**. The two phosphorus-containing ligands lie approximately *cis* to one another $[\text{P}(1)\text{-Fe}(1)\text{-P}(2) 96.25(3)^\circ]$, $[\text{P}(1)\text{-Fe}(1)\text{-P}(3) 113.11(3)^\circ]$. Thus the Fe(1) center can be considered to possess a distorted trigonal bipyramidal coordination geometry with P(2) and C(2) occupying axial sites $[\text{P}(2)\text{-Fe}(1)\text{-C}(2) 174.63(9)^\circ]$ and P(1), P(3) and C(1) lying in the equatorial plane. We call this geometry *cis* (ax–eq) (Scheme 5) as the cyclometallated phosphorus and phosphido groups lie *cis* to one another while the phosphorus atoms of the diphosphine occupy axial and equatorial sites. An alternative conformation is *trans* (eq–eq) and here the cyclometallated

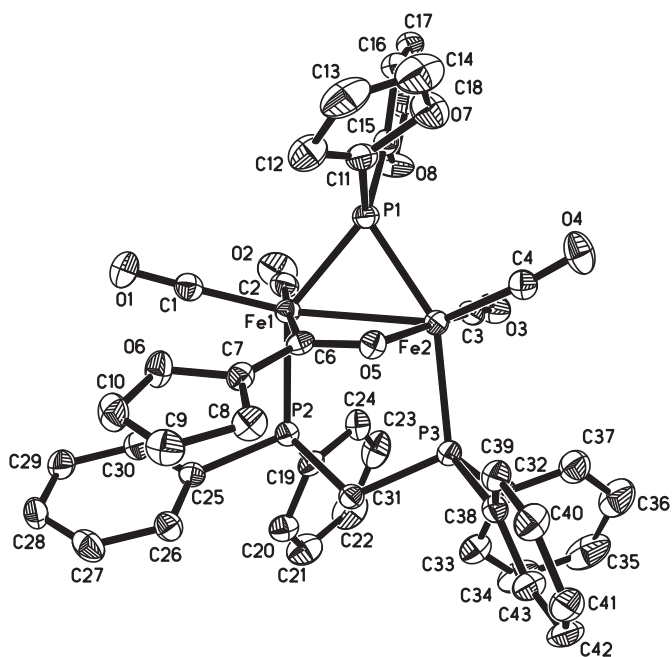
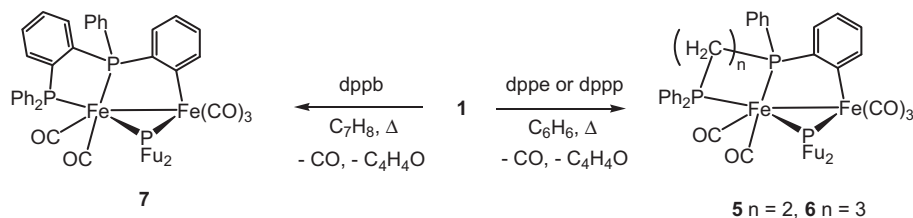


Fig. 2. Molecular structure of $[\text{Fe}_2(\text{CO})_4(\mu\text{-dppm})(\mu\text{-O=C-Fu})(\mu\text{-PFu}_2)]$ (**3**) with selected bond lengths (Å) and angles ($^\circ$): Fe(1)–Fe(2) 2.6598(6), Fe(1)–P(1) 2.1894(8), Fe(1)–P(2) 2.2197(8), Fe(2)–P(1) 2.2044(8), Fe(2)–P(3) 2.2554(8), Fe(2)–O(5) 1.998(2), Fe(1)–C(6) 1.935(2), C(6)–O(5) 1.270(3), P(1)–Fe(1)–P(2) 141.80(3), P(1)–Fe(2)–P(3) 152.05(3).



Scheme 4.

phosphorus and phosphido groups subtend a much larger angle. While in the solid-state it is clear that the molecule exists in the *cis* (ax–eq) conformation, this appears not to be the case in solution. Thus the $^{31}\text{P}\{^1\text{H}\}$ NMR spectrum of **5** consists of three sharp multiplets, a doublet of doublets at 101.0 ($J = 134, 15$ Hz) ppm assigned to the phosphido-bridge, a second doublet of doublets at 83.9 ($J = 134, 19$ Hz) ppm and a triplet at 81.0 ($J = 17$ Hz) ppm. The large coupling constant cannot be easily explained on the basis of the observed solid-state structure and is more consistent with a *trans* (eq–eq) conformation. Thus we suggest that the two forms are in equilibrium in solution with the *trans* (eq–eq) conformation being favoured.

Further insight into this dynamic equilibrium comes from close inspection of the $^{31}\text{P}\{^1\text{H}\}$ NMR spectra of the dppe and dppb derivatives **6** and **7**, respectively. For **7**, this consists of three sharp signals – a doublet of doublets at 138.7 ($J = 55, 30$ Hz) ppm assigned to the phosphido-bridge, a second doublets of doublets at 82.7 ($J = 55, 30$ Hz) ppm and an apparent triplet at 90.5 ($J = 55$ Hz) ppm. Thus, it seems that the *cis* (ax–eq) isomer of **7** is prevalent in solution. For the dppp complex **6** the situation is less clear as there is significant broadening of two of the three resonances, consistent with interconversion of isomers at room temperature. Thus, the high-field signal at 31.9 ppm appears as a broad

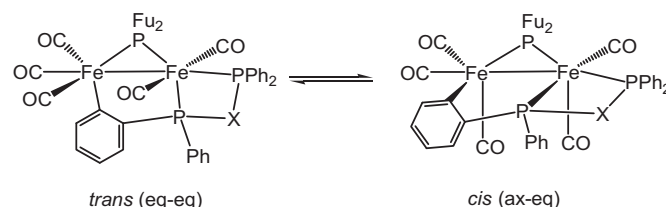
doublet ($J = 116$ Hz), while the two other signals at 73.5 and 56.4 ppm are broadened significantly and no coupling information could be extracted.

Interestingly, Wong and co-workers have reported similar chemistry with $[\text{Ru}_2(\text{CO})_6(\mu\text{-Fu})(\mu\text{-PFu}_2)]$ (**1-Ru**), and both dppe- and dppp-derived complexes, $[\text{Ru}_2(\text{CO})_5\{\mu, \kappa^2\text{-C}_6\text{H}_4\text{PPh}(\text{CH}_2)_n\text{PPh}_2\}(\mu\text{-PFu}_2)]$ ($n = 2\text{--}3$) have been crystallographically characterized [21]. Both adopt the *cis* (ax–eq) conformation found for **5** in the solid-state, although in solution they show quite different $^{31}\text{P}\{^1\text{H}\}$ NMR spectra. Thus, the dppe-derived complex is characterized by phosphorus–phosphorus coupling constants of 124, 25 and 25 Hz, while for the dppp-derived complex the three coupling constants are 38, 31 and 4 Hz. This data supports the postulated equilibrium between the two isomers (Scheme 5) and also suggests that the *cis* (ax–eq) isomer is favoured in the solid-state.

The mode of formation of the cyclometallated complexes **5–7** remains unclear but, based on the facile nature of the carbonyl insertion noted upon reaction of **1** with dppm and dppn, we favour a process in which species akin to **4** are now intermediates. Oxidative addition of a carbon–hydrogen bond to the diiron unit could be facilitated by switching of the furyl–acyl ligand from a bridging to a monodentate coordination mode *via* cleavage of the iron–oxygen bond with subsequent elimination of furan, resulting in formation of the observed products. The high volatility of furan makes it difficult to show that this is indeed eliminated. The relatively flexible nature of the methylene backbones in dppe and dppp might be expected to facilitate such a transformation, and the relatively high yield obtained for the dppb product **7** suggests that it is predisposed to cyclometallation. The dppn complex **4** does not appear to undergo cyclometallation and we speculate that this may be a consequence of the extremely bulky and inflexible nature of the naphthalene linking unit which does not allow close approach of a phenyl group to the diiron center.

3.4. Reaction of **1** with bis(diphenylphosphino)-1,1'-binaphthalene (BINAP) – unexpected formation of the triphosphine complex $[\text{Fe}_2(\text{CO})_5\{\mu, \kappa^3\text{-C}_6\text{H}_4\text{P}(\text{C}_{20}\text{H}_{12}\text{PPh}_2)_2\text{C}_6\text{H}_4\text{PFu}\}]$ (**8**)

Over the past two decades, BINAP has found widespread in transition metal chemistry [22] but it is only relatively recently that the coordination chemistry of this ligand at polynuclear metal centers has been reported [23]. Heating **1** and BINAP in toluene for 24 h resulted in the isolation of the new triphosphine complex



Scheme 5.

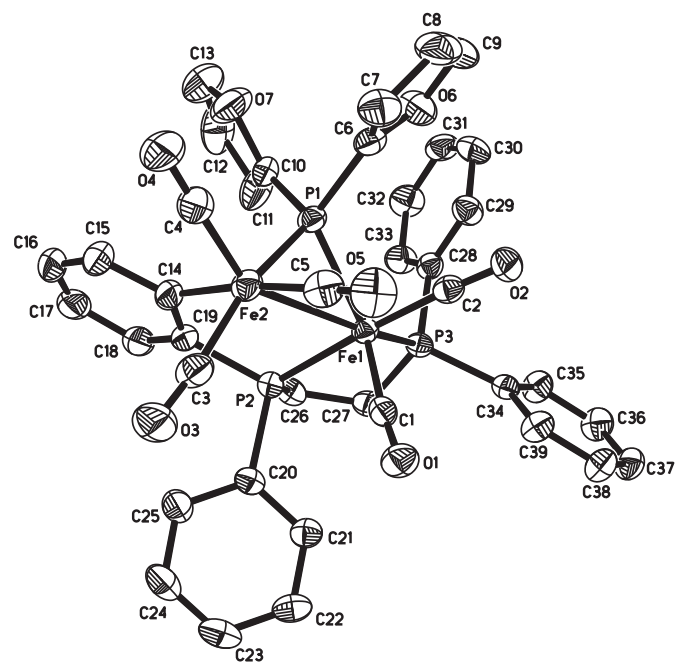
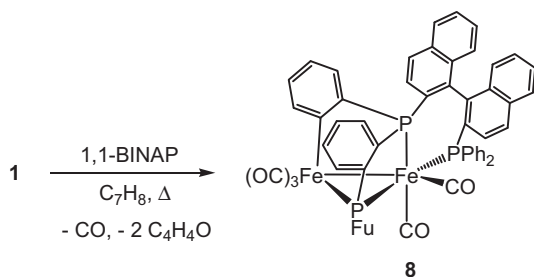


Fig. 3. Molecular structure of $[\text{Fe}_2(\text{CO})_5\{\mu, \kappa^2\text{-C}_6\text{H}_4\text{PPh}(\text{CH}_2)_2\text{PPh}_2\}(\mu\text{-PFu}_2)]$ (**5**) with selected bond lengths (Å) and angles ($^\circ$): Fe(1)–Fe(2) 2.7639(6), Fe(1)–P(1) 2.2199(9), Fe(1)–P(2) 2.24369(9), Fe(1)–P(3) 2.2198(81), Fe(2)–P(1) 2.2023(9), Fe(2)–C(14) 2.042(3), P(1)–Fe(1)–P(2) 96.25(3), P(1)–Fe(1)–P(3) 113.11(3), P(2)–Fe(1)–P(3) 85.28(3), P(1)–Fe(2)–C(14) 85.60(9).



Scheme 6.

$[\text{Fe}_2(\text{CO})_5(\mu, \kappa^3\text{-C}_6\text{H}_4\text{P}(\text{C}_{20}\text{H}_{12}\text{PPh}_2)\text{C}_6\text{H}_4\text{PFu})]$ (**8**) in 18% yield after workup (Scheme 6). Characterization of **8** relied heavily on a single crystal X-ray diffraction study, the results of which are summarized in Fig. 4 and its caption.

The structure is somewhat related to that of **5** but in **8** both phenyl rings on one phosphorus atom have been metallated. The first phenyl moiety links across to the second iron center as seen in **5** but the other is now linked to a furylphosphido moiety via formation of a new carbon–phosphorus bond and (the putative) loss of a second equivalent of furan. The BINAP-derived part of the new triphosphine chelates to one iron atom [P(1)–Fe(1)–P(2) 89.71(4)°], while the new phosphido moiety still spans the metal–metal bond [Fe(1)–P(3)–Fe(2) 82.26(4)°], the latter being significantly elongated [Fe(1)–Fe(2) 2.8668(7) Å]. The remaining diphenylphosphino group lies approximately *trans* to the phosphido-bridge [P(1)–Fe(1)–P(3) 152.08(4)°], while the central phosphorus atom lies approximately *cis* [P(2)–Fe(1)–P(3) 80.37(4)°]. Overall, the new phosphine donates eight electrons to the diiron center through the three phosphorus atoms and the orthometalated ring [Fe(2)–C(53) 2.073(3) Å].

The coordination geometry at the Fe(1) is now best described as a distorted square-based pyramid in which CO(1) occupies the axial site; thus, C(1) subtends angles at Fe(1) of 109.0(1), 89.2(1), 97.0(1) and 89.4(2)° with P(1), P(2), P(3) and C(2), respectively, while P(2) lies *trans* to C(2) [P(1)–Fe(1)–C(2) 176.3(1)°] and P(1) *trans* to P(3) [P(1)–Fe(1)–P(3) 150.08(4)°]. Spectroscopic data again suggest some degree of flexibility in solution. Thus, the $^{31}\text{P}\{^1\text{H}\}$ NMR

spectrum consists of three well-resolved signals, the new phosphido-bridge appearing as a doublet of doublets at 154.4 ($J = 57, 34$ Hz) ppm and the modified BINAP ligand as a doublet of doublets at 90.7 ($J = 57, 34$ Hz) and an apparent triplet at 64.4 ($J = 57$ Hz) ppm. Given the solid state structure, a large coupling constant might be expected between the phosphorus atoms P(1) and P(3) and the lack of such a coupling suggests that this structure is not maintained in solution. The predominance in solution of an isomer in which the diphenylphosphino moiety occupies the axial site (approximately parallel to the iron–iron vector), with all three phosphorus atoms lying approximately *cis* to one another, would be more in accord with the NMR data.

As far as we are aware, the metallation of BINAP as seen in **8** has not previously been reported. Although orthometallation of phenylphosphines is well-established, BINAP is a very robust ligand that retains its integrity under a wide range of conditions. There are a number of reports of BINAP degradation under catalytic conditions. In a few instances, especially at ruthenium(II) centers, cleavage of a diphenylphosphino moiety has been documented [24].

3.5. Overall reaction scheme

From reactions of $[\text{Fe}_2(\text{CO})_6(\mu\text{-Fu})(\mu\text{-PFu}_2)]$ (**1**) with various phosphines we have isolated five different product types and in seeking to understand how they are interrelated we favour a scenario outlined in Scheme 7. In all reactions it seems likely that initial carbonyl substitution occurs to give the pentacarbonyl complexes $[\text{Fe}_2(\text{CO})_5(\text{phosphine})(\mu\text{-Fu})(\mu\text{-PFu}_2)]$ as characterized here for PPh_3 (complex **2**) and previously shown for PFu_3 [2]. The relatively forcing conditions required to bring about this transformation (heating at $> 80^\circ\text{C}$) are in stark contrast to the behaviour noted for the analogous diruthenium complex that undergoes substitution at room temperature [4]. We believe this points towards a dissociative mechanism operating for **1**, the associative mechanism shown to occur for **1-Ru** [13] being less favourable either due to the smaller size of iron vs ruthenium or the tighter binding of the furyl ligand, which precludes formation of the η^1 -state that is proposed for **1-Ru** [13].

From this state, a second carbonyl substitution could potentially occur to yield complexes of the type $[\text{Fe}_2(\text{CO})_4(\text{phosphine})_2(\mu\text{-Fu})(\mu\text{-PFu}_2)]$.

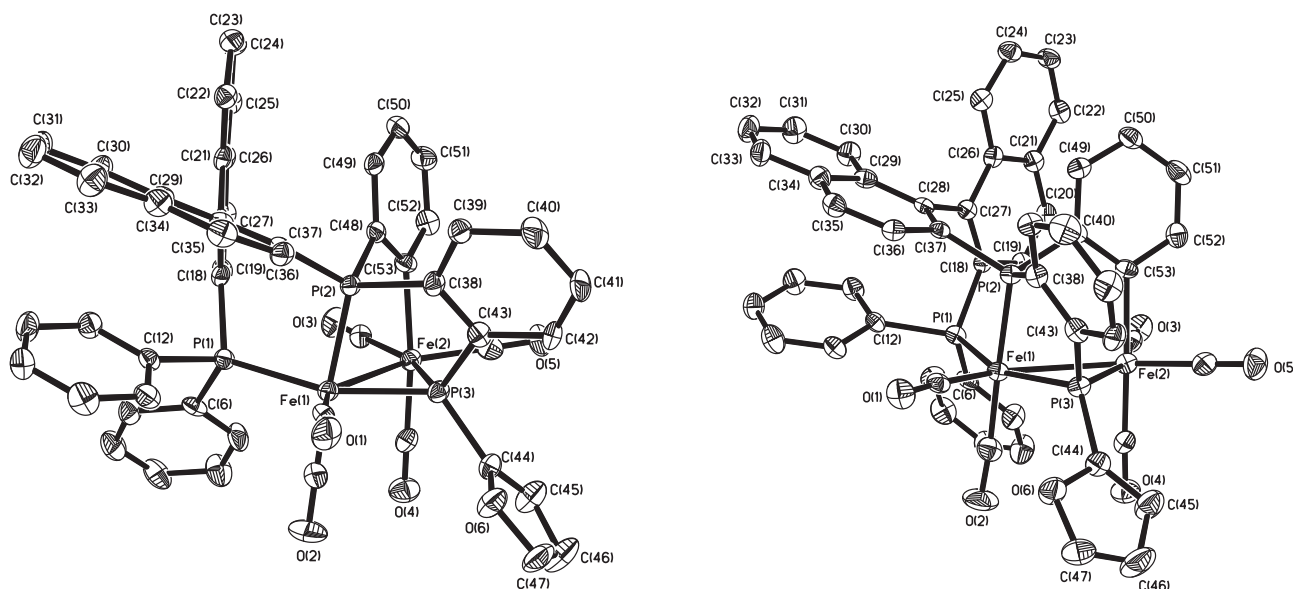
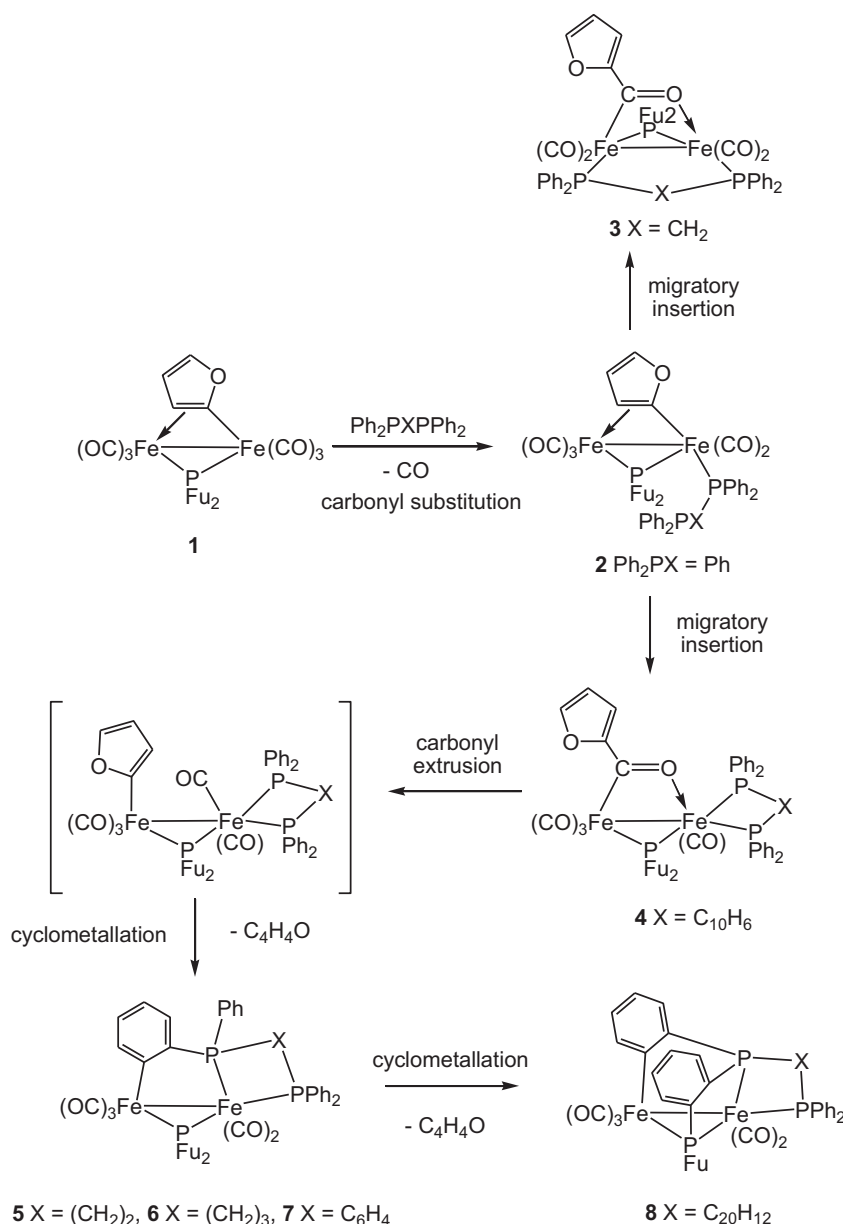


Fig. 4. Two views of the molecular structure of $[\text{Fe}_2(\text{CO})_5(\mu, \kappa^3\text{-C}_6\text{H}_4\text{P}(\text{C}_{20}\text{H}_{12}\text{PPh}_2)\text{C}_6\text{H}_4\text{PFu})]$ (**8**) with selected bond lengths (Å) and angles (°): Fe(1)–Fe(2) 2.8668(7), Fe(1)–P(1) 2.278(1), Fe(1)–P(2) 2.207(1), Fe(1)–P(3) 2.168(1), Fe(2)–P(3) 2.190(1), Fe(2)–C(53) 2.073(3), P(1)–Fe(1)–P(2) 89.71(4), P(1)–Fe(1)–P(3) 152.08(4), P(2)–Fe(1)–P(3) 80.37(4).



Scheme 7.

Fu)(μ -PFu₂) or [Fe₂(CO)₄(diphosphine)(μ -Fu)(μ -PFu₂)], but no such complexes have been detected in this investigation. This is in contrast to the reported reactivity of **1-Ru** with PPh₃, which gives a mixture of [Ru₂(CO)₅(PPh₃)(μ -Fu)(μ -PFu₂)] and [Ru₂(CO)₄(PPh₃)₂(μ -Fu)(μ -PFu₂)] when carried out in refluxing toluene [25]. Instead, it appears that at the diiron unit, coordination of the second phosphine moiety (of a diphosphine) promotes migratory carbonyl insertion to give furyl–acyl complexes with the diphosphine either bridging the metal–metal bond (dppm) or coordinating in a chelate manner to the oxygen-bound iron atom (dppn). In the analogous thienyl chemistry, chelating thienyl–acyl complexes [Fe₂(CO)₄(κ^2 -diphosphine)(μ -O=C–Th)(μ -PTh₂)] are formed with a large range of diphosphines, including dppe, dppp and dppb [18]. For **1**, reaction with these diphosphines affords only the cyclometallated complexes **5–7** resulting from the putative elimination of furan. We believe that these complexes are generated *via* furyl–acyl intermediates, in parallel with the analogous thienyl

chemistry, where [Fe₂(CO)₅{ μ , κ^2 -C₆H₄PPh(C₆H₄)PPh₂}(μ -PTh₂)] is formed upon heating [Fe₂(CO)₄(κ^2 -dppb)(μ -O=C–Th)(μ -PTh₂)] in toluene [18]. We favour a process that proceeds *via* initial carbonyl extrusion to afford a species (shown in Scheme 7) with a terminally bonded furyl ligand, in keeping with maintaining the 34-electron count, but cannot rule out an intermediate with a bridging furyl moiety and no metal–metal bond, which also fulfils the latter criterion. Oxidative addition of a phenyl ring to the second metal atom and subsequent elimination of furan would then give the isolated cyclometallated complexes **5–7**. As discussed earlier, isolation of the furyl–acyl complex **4** suggests that such a process is less facile for the dppn ligand and we attribute this to the larger steric bulk of this ligand that precludes close approach to the diiron center of the phenyl groups.

In the case of 1,1-BINAP, a second equivalent of furan is putatively eliminated to yield the isolated triphosphine (diphosphine–phosphide) complex **8**. The BINAP ligand is very bulky but, unlike

dppn, the backbone is highly flexible and presumably allows for close approach of one or more phenyl rings to the binuclear center. We favour a scenario whereby **8** forms via an intermediate of the type **5–7**. Formation of **8** also requires cleavage of a furyl group from the difurylphosphido ligand. Although this is unusual, it is not unprecedented. Thus, in recent work we have shown that $[(\mu\text{-H})\text{Ru}_3(\text{CO})_7(\mu\text{-dppm})(\mu_3\text{-C}_4\text{H}_2\text{O})(\mu\text{-PFu}_2)]$ transforms into the phosphinidene cluster $[\text{Ru}_3(\text{CO})_7(\mu\text{-dppm})(\mu_3\text{-C}_4\text{H}_2\text{O})(\mu_3\text{-PFu})]$ in 70% yield in refluxing toluene [26]. It is not appropriate to speculate how this might happen at the diiron center, and putative elimination of furan and formation of a new carbon-phosphorus bond are also required for the formation of **8**. Nevertheless the basic framework is very similar to those found in **5–7**, suggesting that this structural unit is thermodynamically favoured at the diiron center.

4. Summary and conclusions

Reaction of the σ,π -furyl complex $[\text{Fe}_2(\text{CO})_6(\mu\text{-Fu})(\mu\text{-PFu}_2)]$ (**1**) with mono- or diphosphines at relatively elevated temperatures (80 °C) does not only lead to direct ligand substitution (phosphine replacing carbonyl) but also, in the case of diphosphines, activation of the coordinating diphosphine as well as the bridging furyl and/or difurylphosphido units of **1**. When both phosphine moieties of the diphosphines dppm or dppn coordinate – to let the diphosphine bridge the Fe–Fe bond (dppm) or chelate one iron atom (dppn) – carbonyl displacement leading to migratory insertion of the carbonyl into a metal–furyl bond occurs, giving a bridging furyl–acyl unit. For the diphosphines dppe, dppp and dppb, the diphosphine coordinates to one iron while a phenyl moiety of the diphosphine is orthometallated, leading to diiron complexes from which the bridging furyl moiety has been eliminated (presumably as furan – furyl + hydride). In what we believe to be an unprecedented reaction for the diphosphine BINAP, the reaction with **1** leads both to orthometallation of a BINAP phenyl moiety and the formation of a carbon-phosphorus bond between a second phenyl moiety and the bridging difurylphosphido moiety of **1**; both processes do presumably proceed via elimination of furan (furyl plus hydride).

The diiron complex **1** exhibits substitution chemistry that is markedly different from its diruthenium analogue **1-Ru** [12,13,21]. For the monodentate phosphine triphenylphosphine, only a trace of disubstituted product could be detected in the case of **1**, in contrast to the reaction with **1-Ru** in refluxing toluene, which led to the formation of both mono- and disubstituted products. Furthermore, phosphine substitution on **1-Ru** occurs at room temperature in an associative reaction [13], whereas phosphine substitution on **1** only takes place at elevated temperatures, suggesting that dissociation of a carbonyl ligand may be the rate-limiting step in the substitution process. In the case of reaction of **1** with dppm, a furyl–acyl moiety is formed, whereas reaction of the same diphosphine with **1-Ru** yields a bridging dppm ligand which may be the result of direct substitution of two carbonyl ligands. On the other hand, the reactions of **1** and **1-Ru** with dppe and dppp parallel each other, giving the same kind of products (*vide supra*).

Acknowledgements

This research has been part sponsored by the Ministry of Education, Government of the People's Republic of Bangladesh. We thank the European Union (Erasmus Mundus) and the Commonwealth Scholarship Commission for scholarships to AR and SG respectively. We also thank Professor Brian K. Nicholson for recording mass spectra and Dr Abdul Mottalib for recording some of the NMR spectra.

Appendix A. Supplementary material

CCDC 932550–932553 contain the supplementary crystallographic data for this paper. These data can be obtained free of charge from The Cambridge Crystallographic Data Centre via www.ccdc.cam.ac.uk/data_request/cif.

References

- See for example: (a) V. Farina, *Pure Appl. Chem.* 68 (1996) 73–78; (b) W.-Y. Wong, F.-L. Ting, Z. Lin, *Organometallics* 22 (2003) 5100–5108; (c) N.G. Anderson, B.A. Keay, *Chem. Rev.* 101 (2001) 997–1030; (d) M. Sakai, H. Hayashi, N. Miyaura, *Organometallics* 16 (1997) 4229–4231; (e) E. Shirakawa, K. Yamasaki, T. Hiyama, *Synthesis* (1998) 1544–1549; (f) B.M. Trost, Y.H. Rhee, *J. Am. Chem. Soc.* 121 (1999) 11680–11683; (g) J.C. Anderson, H. Namli, C.A. Roberts, *Tetrahedron* 53 (1997) 15123–15134; (h) S. Ghosh, M. Khatun, D.T. Haworth, S.V. Lindeman, T.A. Siddiquee, D.W. Bennett, G. Hogarth, E. Nordlander, S.E. Kabir, *J. Organomet. Chem.* 694 (2009) 2941–2948; (i) S. Karmaker, S. Ghosh, S.E. Kabir, D.T. Haworth, S.V. Lindeman, *Inorg. Chim. Acta* 382 (2012) 199–202; (j) Md.A. Rahman, N. Begum, S. Ghosh, Md. K. Hossain, G. Hogarth, D.A. Tocher, E. Nordlander, S.E. Kabir, *J. Organomet. Chem.* 696 (2011) 607–612; (k) C. Santelli-Rouvier, C. Coin, L. Toupet, M. Santelli, *J. Organomet. Chem.* 495 (1995) 91–96; (l) W.-Y. Wong, F.-L. Ting, Y. Guo, Z. Lin, *J. Cluster Sci.* 16 (2005) 185–200; (m) S. Ghosh, G. Hogarth, S.E. Kabir, E. Nordlander, L. Salassa, D.A. Tocher, *J. Organomet. Chem.* 696 (2011) 1982–1989; (n) M.I. Hossain, M.D.H. Sikder, S. Ghosh, S.E. Kabir, G. Hogarth, L. Salassa, *Organometallics* 31 (2012) 2546–2558; (o) S. Ghosh, S. Rana, D.A. Tocher, G. Hogarth, E. Nordlander, S.E. Kabir, *J. Organomet. Chem.* 694 (2009) 3312–3319; (p) W.-Y. Wong, F.-L. Ting, Y. Guo, Z. Lin, *J. Cluster Sci.* 19 (2008) 231–245.
- A. Rahaman, F. Rafiqul Alam, S. Ghosh, M. Haukka, S.E. Kabir, E. Nordlander, G. Hogarth, *J. Organomet. Chem.* 730 (2013) 123–131.
- W.-Y. Wong, F.-L. Ting, W.-L. Lam, *J. Chem. Soc. Dalton Trans.* (2001) 2981–2988.
- N. Begum, M.A. Rahman, M.R. Hassan, D.A. Tocher, E. Nordlander, G. Hogarth, S.E. Kabir, *J. Organomet. Chem.* 693 (2008) 1645–1655.
- SAINT Software for CCD Diffractometer, V.7.23A, Bruker AXS, 2005.
- G.M. Sheldrick, SADABS – Bruker Nonius Scaling and Absorption Correction, Bruker AXS, Inc., Madison, Wisconsin, USA, 2008.
- Bruker AXS, APEX2-Software Suite for Crystallographic Programs, Bruker AXS, Inc., Madison, WI, USA, 2009.
- G.M. Sheldrick, SHELXS-86, Program for Crystal Structure Determination, University of Göttingen, Göttingen, Germany, 1986.
- G.M. Sheldrick, *Acta Crystallogr.* A64 (2008) 112–122.
- L.J. Farrugia, *J. Appl. Crystallogr.* 32 (1999) 837–838.
- A.L. Spek, A Multipurpose Crystallographic Tool, Utrecht University, Utrecht, The Netherlands, 2003.
- M.K. Anwar, G. Hogarth, O.S. Senturk, W. Clegg, S. Doherty, M.R.J. Elsegood, *J. Chem. Soc. Dalton Trans.* (2001) 341–352.
- G. Hogarth, S. Ghosh, S.E. Kabir, unpublished results.
- (a) D. Seyferth, J.B. Hoke, J.C. Dewan, P. Hofmann, M. Schnellbach, *Organometallics* 13 (1994) 3452–3464; (b) D. Seyferth, C.M. Archer, D.P. Ruschke, M. Cowie, R.W. Hilt, *Organometallics* 10 (1991) 3363–3380; (c) J.B. Hoke, J.C. Dewan, D. Seyferth, *Organometallics* 6 (1987) 1816–1819; (d) D. Seyferth, J.B. Hoke, G.B. Womack, *Organometallics* 9 (1990) 2662–2672; (e) D. Seyferth, K.S. Brewer, T.G. Wood, M. Cowie, R.W. Hilt, *Organometallics* 11 (1992) 2570–2579; (f) L. Song, J. Liu, J. Wang, *Huaxue Xuebao* 48 (1990) 110–115; (g) L. Song, R. Wang, Q. Hu, H. Wang, *Jiegou Huaxue* 8 (1989) 115–118.
- (a) G. Hogarth, M.H. Lavender, K. Shukri, *J. Organomet. Chem.* 527 (1997) 247–258; (b) S. Doherty, G. Hogarth, M. Waugh, T.H. Scanlan, M.R.J. Elsegood, W. Clegg, *J. Organomet. Chem.* 620 (2001) 150–164; (c) G. Hogarth, M. O'Brien, D.A. Tocher, *J. Organomet. Chem.* 672 (2003) 22–28; (d) S. Doherty, G. Hogarth, M.R.J. Elsegood, W. Clegg, N.H. Rees, M. Waugh, *Organometallics* 17 (1998) 3331–3345; (e) S. Doherty, G. Hogarth, *Inorg. Chem. Commun.* 1 (1998) 257–259.
- S.R. Gilbertson, X. Zhao, D.P. Dawson, K.L. Marshall, *J. Am. Chem. Soc.* 115 (1993) 8517–8518.
- G. Hogarth, K. Shukri, S. Doherty, A.J. Carty, G.D. Enright, *Inorg. Chim. Acta* 291 (1999) 178–189.
- A. Rahaman, F. Rafiqul Alam, S. Ghosh, D.A. Tocher, M. Haukka, S.E. Kabir, E. Nordlander, G. Hogarth, in press.
- (a) R.J. Puddephatt, *Chem. Soc. Rev.* (1983) 99–127; (b) B. Chaudret, B. Delavaux, R. Poilblanc, *Coord. Chem. Rev.* 86 (1988) 191–243.

- [20] (a) S. Ghosh, G. Hogarth, S.E. Kabir, A.L. Miah, L. Salassa, S. Sultana, C. Garino, *Organometallics* 28 (2009) 7047–7052;
(b) S.E. Kabir, F. Ahmed, S. Ghosh, Md.R. Hassan, Md.S. Islam, A. Sharmin, D.A. Tocher, D.T. Haworth, S.V. Lindeman, T.A. Siddiquee, D.W. Bennett, K.I. Hardcastle, *J. Organomet. Chem.* 693 (2008) 2657–2665;
(c) V.N. Nesterov, W.H. Watson, S. Kandala, M.G. Richmond, *Polyhedron* 26 (2007) 3602–3608;
(d) C. Taouss, P.G. Jones, *Dalton Trans.* 40 (2011) 11687–11689;
(e) S.L. James, A.G. Orpen, P.G. Pringle, *J. Organomet. Chem.* 525 (1996) 299–301.
- [21] W.-Y. Wong, F.-L. Ting, W.-L. Lam, *Eur. J. Inorg. Chem.* (2002) 2103–2111.
- [22] (a) T. Ohkuma, N. Kurono, *Privileged Chiral Ligands Catal.* (2011) 1–53;
(b) S. Akutagawa, *Appl. Catal. A* 128 (1995) 171–207.
- [23] (a) S.E. Gibson, D.J. Hardick, P.R. Haycock, K.A.C. Kaufmann, A. Miyazaki, M.J. Tozer, A.J.P. White, *Chem. Eur. J.* 13 (2007) 7099–7109;
(b) S.E. Gibson, K.A.C. Kaufmann, P.R. Haycock, A.J.P. White, D.J. Hardick, M.J. Tozer, *Organometallics* 26 (2007) 1578–1580;
(c) S.E. Gibson, K.A.C. Kaufmann, J.A. Loch, J.W. Steed, A.J.P. White, *Chem. Eur. J.* 11 (2005) 2566–2576;
(d) S.E. Gibson, S.E. Lewis, J.A. Loch, J.W. Steed, M.J. Tozer, *Organometallics* 22 (2003) 5382–5384;
(e) M.J. Stchedroff, V. Moberg, E. Rodriguez, A.E. Aliev, J. Böttcher, J.W. Steed, E. Nordlander, M. Monari, A.J. Deeming, *Inorg. Chim. Acta* 359 (2006) 926–937;
(f) A.J. Deeming, M. Stchedroff, *J. Chem. Soc. Dalton Trans.* (1998) 3819–3824;
(g) A.J. Deeming, D.M. Speel, M. Stchedroff, *Organometallics* 16 (1997) 6004–6009;
(h) S.P. Tunik, T.S. Pilyugina, I.O. Koshevoy, S.I. Selivanov, M. Haukka, T.A. Pakkanen, *Organometallics* 23 (2004) 568–579;
(i) F. Prestopino, R. Persson, M. Monari, N. Focci, E. Nordlander, *Inorg. Chem. Commun.* 1 (1998) 302–304.
- [24] (a) L.M. Alcazar-Roman, J.F. Hartwig, A.L. Rheingold, L.M. Liable-Sands, I.A. Guzei, *J. Am. Chem. Soc.* 122 (2000) 4618–4630;
(b) T. Geldbach, P.S. Pregosin, M. Bassetti, *Organometallics* 20 (2001) 2990–2997;
(c) C.J. den Reijer, M. Woerle, P.S. Pregosin, *Organometallics* 19 (2000) 309–316;
(d) T.J. Geldbach, F. Breher, V. Gramlich, P.G.A. Kumar, P.S. Pregosin, *Inorg. Chem.* 43 (2004) 1920–1928;
(e) T.J. Geldbach, P.S. Pregosin, A. Albinati, *Organometallics* 22 (2003) 1443–1451.
- [25] W.-Y. Wong, F.-L. Ting, W.-L. Lam, *Open J. Inorg. Chem.* 2 (2008) 50–55.
- [26] Md.N. Uddin, N. Begum, M.R. Hassan, G. Hogarth, S.E. Kabir, Md.A. Miah, E. Nordlander, D.A. Tocher, *Dalton Trans.* (2008) 6219–6230.